Magnetic compensation of gravity forces in liquid/gas mixtures: surpassing intrinsic limitations of a superconducting magnet by using ferromagnetic inserts

Quettier Lionel[1,*], Félice Hélène[1,*], Mailfert Alain[2], Chatain Denis[3], and Beysens Daniel[3]

[1] GREEN, INPL-Nancy, 2 Av. de la Forêt de Haye, F-54516 Vandoeuvre, France.

[*] now with SACM, CEA-Saclay, F-91191 Gif-sur-Yvette, France.

[2] LEM, INPL-Nancy, 2 Av. de la Forêt de Haye, F-54516 Vandoeuvre, France.

and

[3] SBT, CEA-Grenoble, 17 Rue des Martyrs, F-38054 Grenoble Cedex, France.

Abstract. Magnetic compensation of gravity forces, similar to the space conditions of "microgravity", needs the production of a uniform magnetic force field. We derive here a basic mathematical result that shows the impossibility to establish exact gravity compensation in a finite volume. The imperfection of compensation can be, however, quantified and a relation is derived between homogeneity accuracy and compensation volume in a cylindrical symmetry. We study how the use of inserts made of saturated ferromagnetic materials can modify the homogeneity of magnetic force field. In order to illustrate this result, an iron insert has been numerically calculated for the particular case of gravity compensation of H_2 in a 10 T superconducting coil. An experimental test has been carried out on a H_2 vapour bubble very close to its gas-liquid critical point. Near the critical point the gas-liquid interfacial tension is vanishing, then any bubble deformation from the ideal spherical shape reveals the non-homogeneities in the magnetic compensation force.

PACS numbers: 85.70.Rp, 84.71.Ba, 64.60.Fr, 68.03-g

1 Introduction

Magnetic compensation of gravity forces ("magnetic levitation") finds one of its most useful applications in recreating some feature of space conditions where weightlessness conditions or "microgravity" prevail. Nowadays, it is not uncommon in biology and fluids physics to levitate organic substances, liquids and solids [1- 3]. Another example can be found in aerospace where studying the behavior of cryopropellants under variable acceleration, including the weightlessness situation, has been envisaged [4]. If it is relatively easy to compensate gravity at the center of mass of a solid body, the same problem with a mixture of gas, liquid and solid materials is much more difficult. Indeed, the magnetic force density must exhibit the same degree of homogeneity than the earth gravity field.

The principle of magnetic levitation in static magnetic field is based on the compensation of gravity by applying to a pure material a magnetic volumic force directed antiparallel to the gravity force. The material can exhibit different phases (gas, liquid, solid) but with the same specific magnetic susceptibility. In practice, this condition limits the use of this technique to the different phases of a pure substance. The phases can be at coexistence or not, at equilibrium or not.

If a small volume V of material under the magnetic field $\vec{H}$ is considered, this magnetic force $\vec{F}_m$ is given by:

$$\vec{F}_m = \frac{1}{2} V \chi_m \mu_0 \overrightarrow{\text{grad}}\left(\vec{H}^2\right) \tag{1}$$

where μ_0 is the magnetic permeability of vacuum and χ_m the magnetic susceptibility of the material.

To produce a force that can compensate gravity, a vector field $\vec{G} = \overrightarrow{\text{grad}}(\vec{B}^2)$ is needed, where $\vec{B} = \mu_0 \vec{H}$ is the applied magnetic flux density. The following values of G, $G \sim$ 2800 T^2/m, 1000 T^2/m and 2000 T^2/m are necessary to achieve respectively the compensation in Water, Hydrogen (H_2) and Deuterium. High B value and high spatial variation of B are then needed to reach these G values with a good homogeneity in a useful volume of at least several mm^3. These conditions can be obtained near the ends of superconducting magnets or hybrids coils [1-3, 5-6] or, as suggested and tested in [7], in associating ferromagnetic materials with superconducting coils.

This paper is organized as follows. In the first part, important theoretical results concerning the vector field $\overrightarrow{\text{grad}}(\vec{B}^2)$ are presented. Then, in order to modify the magnetic force field homogeneity preexisting in a solenoid, a model of particular ferromagnetic insert is derived. In the last section, some experimental results about the shape of a H_2 bubble very near its critical point obtained with and without insert are presented.

2 Some properties of the vector field $\overrightarrow{\text{grad}}(\vec{B}^2)$

Although there has been till now many applications in science and technology of magnetic forces, no particular studies of magnetic vector force field has been performed so far. In this section, some mathematical and physical properties of the vector field $\overrightarrow{\text{grad}}(\vec{B}^2)$ are introduced.

2.1 Theorem: of the impossibility to create a uniform vector field $\overrightarrow{\text{grad}}(\vec{B}^2)$

The aim of the demonstration is to prove the followings: if $\vec{B}$ defines a magnetic flux density, the vector $\overrightarrow{\text{grad}}(B^2)$ cannot be at the same time constant and non zero.

Here the space vector $\Re^3$ is considered, with the basis formed by the unit vectors $\{\vec{u}_x, \vec{u}_y, \vec{u}_z\}$, in which $\vec{B}$ can be written

$$\vec{B} = B_x(x,y,z)\vec{u}_x + B_y(x,y,z)\vec{u}_y + B_z(x,y,z)\vec{u}_z \tag{2}$$

If $\overrightarrow{\text{grad}}(\vec{B}^2) = \vec{c}$, where $\vec{c}$ is a constant vector, then $\text{div}(\overrightarrow{\text{grad}}(\vec{B}^2)) = 0$. (3)

The following equivalence can be written

$$\text{div}(\overrightarrow{\text{grad}}(\vec{B}^2)) = 0 \Leftrightarrow \frac{\partial^2 B^2}{\partial x^2} + \frac{\partial^2 B^2}{\partial y^2} + \frac{\partial^2 B^2}{\partial z^2} = 0 \tag{4}$$

Calculations give

$$\frac{\partial^2 B^2}{\partial x^2} = 2\left[\left(\frac{\partial B_x}{\partial x}\right)^2 + B_x\frac{\partial^2 B_x}{\partial x^2} + \left(\frac{\partial B_y}{\partial x}\right)^2 + B_y\frac{\partial^2 B_y}{\partial x^2} + \left(\frac{\partial B_z}{\partial x}\right)^2 + B_z\frac{\partial^2 B_z}{\partial x^2}\right] \tag{5}$$

With a circular permutation of indices, expressions of $\frac{\partial^2 B^2}{\partial y^2}$ and $\frac{\partial^2 B^2}{\partial z^2}$ can also be obtained.

Then, using the fact that *B* is harmonic, (4) gives:

$$\left(\frac{\partial B_x}{\partial x}\right)^2+\left(\frac{\partial B_x}{\partial y}\right)^2+\left(\frac{\partial B_x}{\partial z}\right)^2+\left(\frac{\partial B_y}{\partial x}\right)^2+\left(\frac{\partial B_y}{\partial y}\right)^2+\left(\frac{\partial B_y}{\partial z}\right)^2$$

$$+\left(\frac{\partial B_z}{\partial x}\right)^2+\left(\frac{\partial B_z}{\partial y}\right)^2+\left(\frac{\partial B_z}{\partial z}\right)^2=0 \qquad (6)$$

A sum of positive terms equal to zero imposes that each term of this sum is null. Then the fact that $\vec{B}^2$ is uniform also implies $\overrightarrow{\text{grad}}(\vec{B}^2)=\vec{0}$.

Therefore a perfect uniform compensation of gravity cannot be performed in a finite volume. However, gravity can be non uniformly compensated in a given volume if some deviations to weightlessness are accepted. The necessary conditions between the accepted variations and the experimental variables are detailed below.

2.2 Relationship between the important variables

In this section, a relation is established between the magnetic flux density, the magnetic force, the size of the area under compensation, the radial and vertical homogeneities of the force. The method is described below. It defines the performances of the magnetic levitation technique.

Let us define $\vec{G}(\vec{X})=\overrightarrow{\text{grad}}(\vec{B}^2)\Big|_{\vec{X}}$ with $\vec{X}$ a vector of $\Re^3$. A useful variable for the magnetic levitation problem is the vector $\vec{\varepsilon}$, « relative error vector of gravity compensation » defined by the relation:

$$\vec{\varepsilon}(\vec{r})=\frac{\vec{G}(\vec{r})-\vec{G}(\vec{0})}{G_0} \quad , \qquad (7)$$

where $\vec{r}$ is the coordinates vector of one close point of $\vec{r} = \vec{0}$, with $\left|\vec{G}(\vec{0})\right| = G_0$.

Previous works on two-dimensional structures invariant by translation have established the relation between G_0, the radius of the area *R*, the horizontal and vertical homogeneities $\varepsilon_x = \left|\vec{\varepsilon}(R\vec{u}_x)\right|$ and $\varepsilon_y = \left|\vec{\varepsilon}(R\vec{u}_y)\right|$, and the norm of the magnetic flux density vector *B* [8]. A relationship has been previously established starting from the formalism using the complex magnetic potential [5]; it was then generalized with any two-dimensional problem invariant by translation, in any point where the vectors $\vec{B}$ and $\overrightarrow{\text{grad}}(\vec{B}^2)$ are either parallel or perpendicular

$$\left|B\right| = \sqrt{\frac{G_0 R}{2\left(\varepsilon_x + \varepsilon_y\right)}} \quad . \tag{8}$$

A close relation can be found between B, G_0, *R*, ε_r and ε_z for the axisymmetric geometries where $\varepsilon_r = \left|\vec{\varepsilon}(R\vec{u}_r)\right|$ defines the radial homogeneity and $\varepsilon_z = \left|\vec{\varepsilon}(R\vec{u}_z)\right|$ the vertical one. This relation was courteously communicated to the authors [9]. The demonstration is based on a series expansion of the components of the magnetic flux density. Thereafter we make the assumption that the exact compensation of the gravity force, for material concerned, takes place at the origin point O with the axis O_z taken as vertical.

For a general three-dimensional case, we have:

$$\vec{G}(x,y,z) = \vec{G}(0,0,0) + x\left.\frac{\partial \vec{G}}{\partial x}\right|_{(0,0,0)} + y\left.\frac{\partial \vec{G}}{\partial y}\right|_{(0,0,0)} + z\left.\frac{\partial \vec{G}}{\partial z}\right|_{(0,0,0)} + \ldots \tag{9}$$

In the reference frame $(O,\vec{u}_r,\vec{u}_\theta,\vec{u}_z)$ and given the symmetry conditions for this kind of geometries $\vec{B}$ can be written:

$$\vec{B} = B_r(r,z)\vec{u}_r + B_z(r,z)\vec{u}_z \quad . \tag{10}$$

In the neighbourhood of point O, the coordinates of the magnetic flux density can be written with an expansion of order 2:

$$B_r(r,z) = B_r(0,0) + \left.\frac{\partial B_r}{\partial r}\right|_{(0,0)} r + \left.\frac{\partial B_r}{\partial z}\right|_{(0,0)} z + \frac{1}{2}\left(\left.\frac{\partial^2 B_r}{\partial r^2}\right|_{(0,0)} r^2 + 2\left.\frac{\partial^2 B_r}{\partial r \partial z}\right|_{(0,0)} rz + \left.\frac{\partial^2 B_r}{\partial z^2}\right|_{(0,0)} z^2 \right) \tag{11}$$

$$B_z(r,z) = B_z(0,0) + \left.\frac{\partial B_z}{\partial r}\right|_{(0,0)} r + \left.\frac{\partial B_z}{\partial z}\right|_{(0,0)} z + \frac{1}{2}\left(\left.\frac{\partial^2 B_z}{\partial r^2}\right|_{(0,0)} r^2 + 2\left.\frac{\partial^2 B_z}{\partial r \partial z}\right|_{(0,0)} rz + \left.\frac{\partial^2 B_z}{\partial z^2}\right|_{(0,0)} z^2 \right) \tag{12}$$

In vacuum, in a space free of currents, the magnetic flux density $\vec{B}$ satisfies $\overrightarrow{\mathrm{rot}}(\vec{B}) = \vec{0}$ and $\mathrm{div}(\vec{B}) = 0$, which yields:

$$\frac{\partial B_r}{\partial z} = \frac{\partial B_z}{\partial r} \tag{13}$$

and

$$B_r + r\left(\frac{\partial B_r}{\partial r} + \frac{\partial B_z}{\partial z}\right) = 0 \quad . \tag{14}$$

Defining $\alpha_i = \left.\frac{1}{i!}\frac{\partial^i B_z}{\partial z^i}\right|_{(0,0)}$, and choosing $\vec{B}$ has the direction $\vec{u}_z$, one can write at the second order:

$$B_r(r,z) = -\frac{1}{2}\alpha_1 r - \alpha_2 rz \tag{15}$$

$$B_z(r,z) = \alpha_0 + \alpha_1 z + \alpha_2\left(z^2 - \frac{r^2}{2}\right) \tag{16}$$

Since

$$\vec{G} = 2\left(B_r\,\overrightarrow{\text{grad}}(B_r) + B_z\,\overrightarrow{\text{grad}}(B_z)\right) \tag{17}$$

At the first order, we get the following expression for $\vec{G}$:

$$\vec{G}(r,z) = \left(\frac{1}{2}\alpha_1^2 - 2\alpha_0\alpha_2\right) r\vec{u}_r + \left(2\alpha_0\alpha_1 + \left(2\alpha_1^2 + 4\alpha_0\alpha_2\right)z\right)\vec{u}_z \quad . \tag{18}$$

The radial and vertical homogeneities at the surface of a spherical domain of radius *R* are then obtained:

$$\varepsilon_r = \frac{\alpha_1^2 - 4\alpha_0\alpha_2}{4\alpha_0\alpha_1} R \tag{19}$$

and

$$\varepsilon_z = \frac{\alpha_1^2 + 2\alpha_0\alpha_2}{\alpha_0\alpha_1} R \quad . \tag{20}$$

As $B_0 = \alpha_0$ and $G_0 = 2\alpha_0\alpha_1$, one finally obtains a relationship between the magnetic flux density B_0, the magnetic force G_0, the size *R* of the area and the radial and vertical homogeneities of the force ε_r and ε_z for an axisymmetric system:

$$B_0 = \frac{1}{2}\sqrt{\frac{3G_0 R}{2\varepsilon_r + \varepsilon_z}} \quad . \tag{21}$$

This relation is very important in practice, as it determines the size of the compensated volume for a given material with the allowed inhomogeneities ε_r and ε_z.

3 Calculation of a ferromagnetic insert for compensation in H_2

3.1 Context

In order to lower the unavoidable force field inhomogeneities, or increase the working volume at given homogeneity, the use of a magnetic insert inside a regular coil is a simple and powerful means. To illustrate this point, we calculate in the following a ferromagnetic insert made of pure iron to modify the magnetic force field created by a superconducting (NbTi) solenoid. This coil can reach 8 T at 4.2 K and 10 T when cooled down at 2.17 K. The useful parameters of the superconducting solenoid are given in Table I.

Tab. I. Parameters of the superconducting solenoid

Inner diameter (mm)	89.5
Outer diameter (mm)	186
Total height (mm)	200
Critical current at 2.17 K (A)	72

Let us define Z_u as the position of the center of the levitation area from the coil centre. Several working areas can be considered if the current in the coil makes possible to reach the required value of *G*. Thereafter, we will only focus on two different working areas: we define the so-called L_{max} case which corresponds to the position Z_u where *G* is

maximum, and the so-called L_{equal} case which corresponds to the position Z_u where $\varepsilon_r = \varepsilon_z$.

We will consider in the following only inserts with a simple shape easy to manufacture. The aim is to obtain homogeneity as low as possible in the L_{equal} case.

3.2 Insert calculation

The numerical calculation of this insert was carried out by using the RADIA software [10]. The ferromagnetic parts are modelled by using a relaxation method; a formulation of Biot and Savart type is used for the superconducting parts. The ferromagnetic insert is meshed and the magnetization of each elementary volume is supposed to be parallel with the field lines. The total magnetic field, sum of the magnetic field produced by each element and the field of the coil is finally calculated. The process is then reiterated until the difference between the magnetic field values calculated for two successive iterations is lower than a preliminary fixed tolerance. This method has the disadvantage of using mesh calculations that produce discontinuities of the magnetic field through the boundaries of each element. However, as the magnetic force is computed outside the magnetic materials and outside the field sources, the influence of the discontinuities is much reduced.

Nevertheless, a sufficient precision for the calculation of the magnetic flux density is necessary to evaluate $\overrightarrow{\text{grad}}(\vec{B}^2)$. In the following calculations, a regular mesh of 40*40*40 elements and a convergence criteria of 10^{-4} on calculated fields were used.

Refining these both parameters did not really improve the precision of the results (<0.1%) whereas the time of calculation was considerably increased.

A parametrical study of the dimensions of the insert leads to a hollow cylinder made of iron (magnetic saturation of 2.16 T). Its geometrical characteristics are listed in Table II.

Tab. II. Dimensions of the insert. The bottom of the insert is placed at 50 mm over the coil centre. The insert centre is located at 70 mm over the coil centre.

Position (mm)	50
Outer radius (mm)	44.5
Height (mm)	40
Inner radius (mm)	28

Without insert, in the L_{max} case, the levitation can be carried out at Z_u = 85 mm from the coil centre with a current density J = 188 A/mm². In the L_{equal} case, Z_u = 90.8 mm with 189.3 A/mm². With insert, the calculations show that it is necessary to increase the current circulating in the coil to perform the levitation. Indeed, in the L_{max} case, levitation is obtained at Z_u = 57.6 mm with a current density of 194.1 A/mm^2 to reach the value of 1000 T²/m; in the L_{equal} case, Z_u = + 62.3 mm and J = 195 A/mm². These parameters are summarized in Table III. Figures 1 and 2 show the influence of the insert on the components of the vector $\overrightarrow{\text{grad}}(\vec{B}^2)$ for the L_{equal} and L_{max} cases.

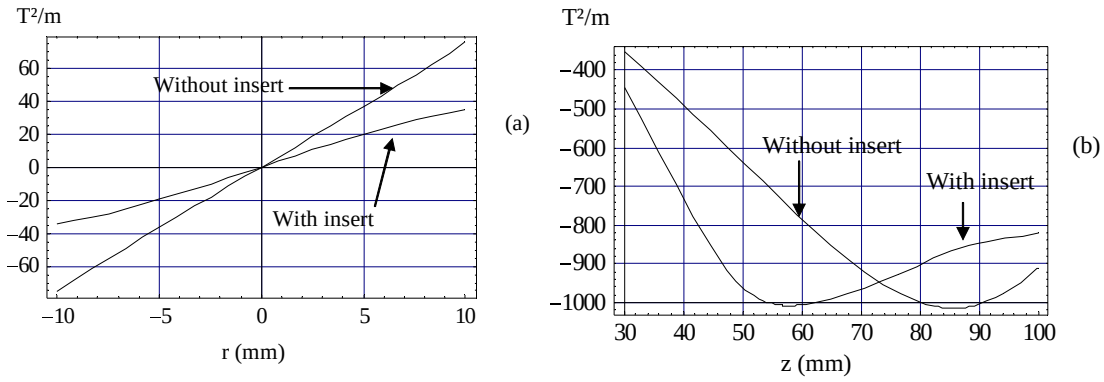

Fig. 1.: L_{equal} case with insert (J = 195 A/mm², Z_u = 62.3 mm) and without insert (J = 189.3 A/mm², Z_u = 90.8 mm). (a) Variation of the radial component of the vector $\overrightarrow{\text{grad}}(\vec{B}^2)$ in T²/m. (b) Variation of the vertical component of the vector $\overrightarrow{\text{grad}}(\vec{B}^2)$ in T²/m on the vertical axis as a function of the distance from the coil centre.

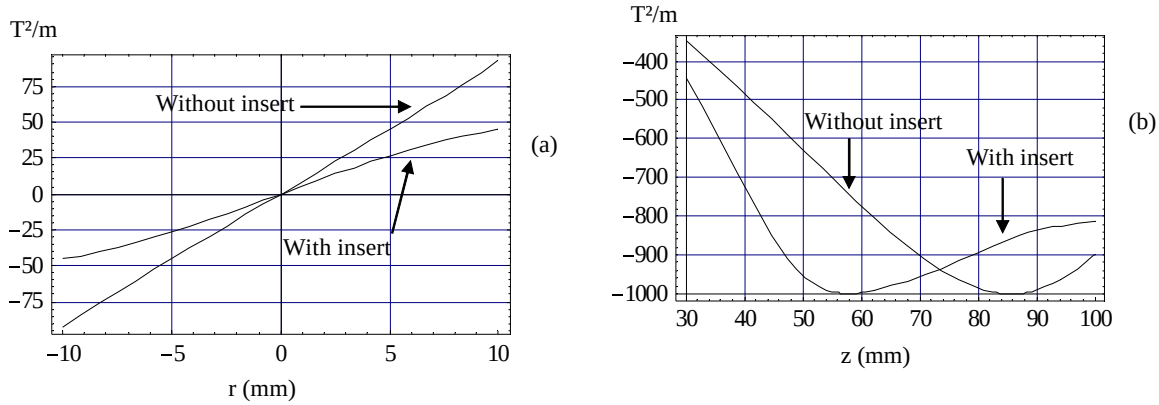

Fig. 2. L_{max} case with insert (J = 194.1 A/mm², Z_u = 57.6 mm) and without insert (J = 188 A/mm², Z_u = 85 mm). (a) Variation of the radial component of the vector $\overrightarrow{\text{grad}}(\vec{B}^2)$ in T²/m. (b) Variation of the vertical component of the vector $\overrightarrow{\text{grad}}(\vec{B}^2)$ in T²/m on the vertical axis as a function of the distance from the coil centre.

Figures 3 and 4 represent the radial and vertical homogeneities of the gravity compensation respectively for L_{equal} and L_{max} cases without and with insert. Spacing of contour lines clearly shows the influence of the insert on the residual force field. Indeed each line corresponds to a variation of 0.25%.

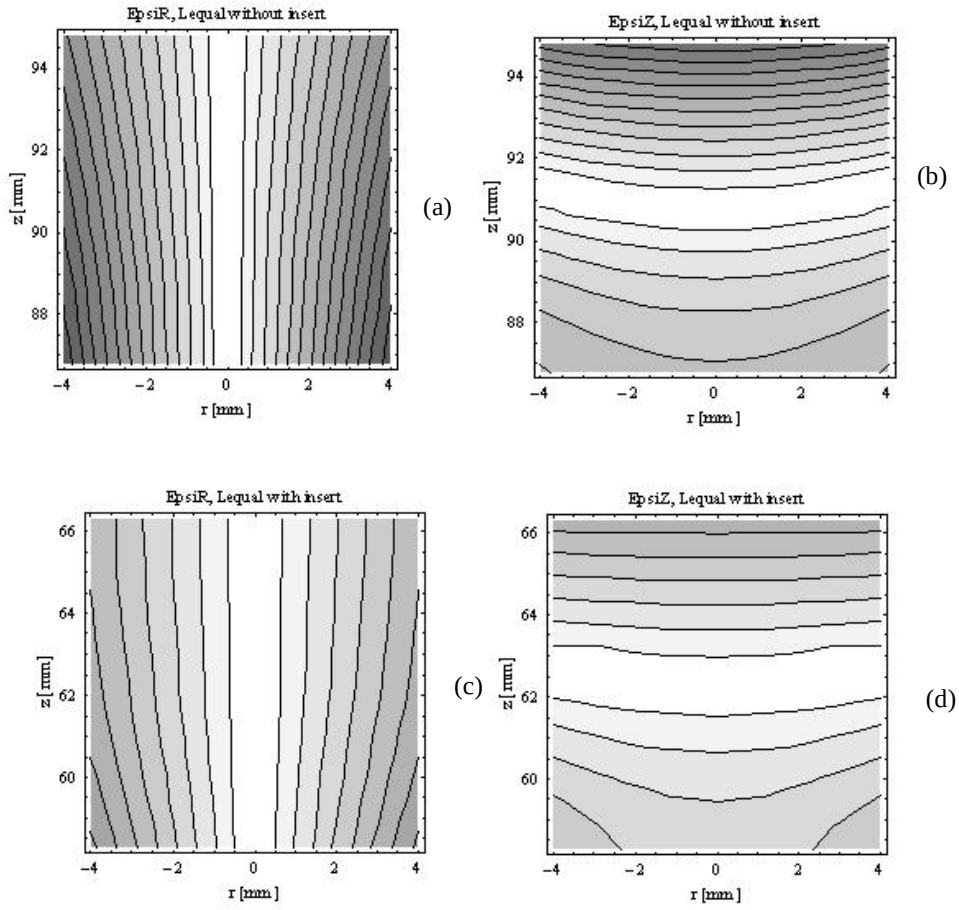

Fig. 3. L_{equal} case: Contour plots of the radial homogeneity ε_r (a) and of the vertical homogeneity ε_z (b) in a window containing the working area without insert (Z_u = 90.8 mm). Contour plots of the radial homogeneity ε_r (c) and of the vertical homogeneity ε_z (d) in a window containing the working area with insert (Z_u = 62.3 mm).

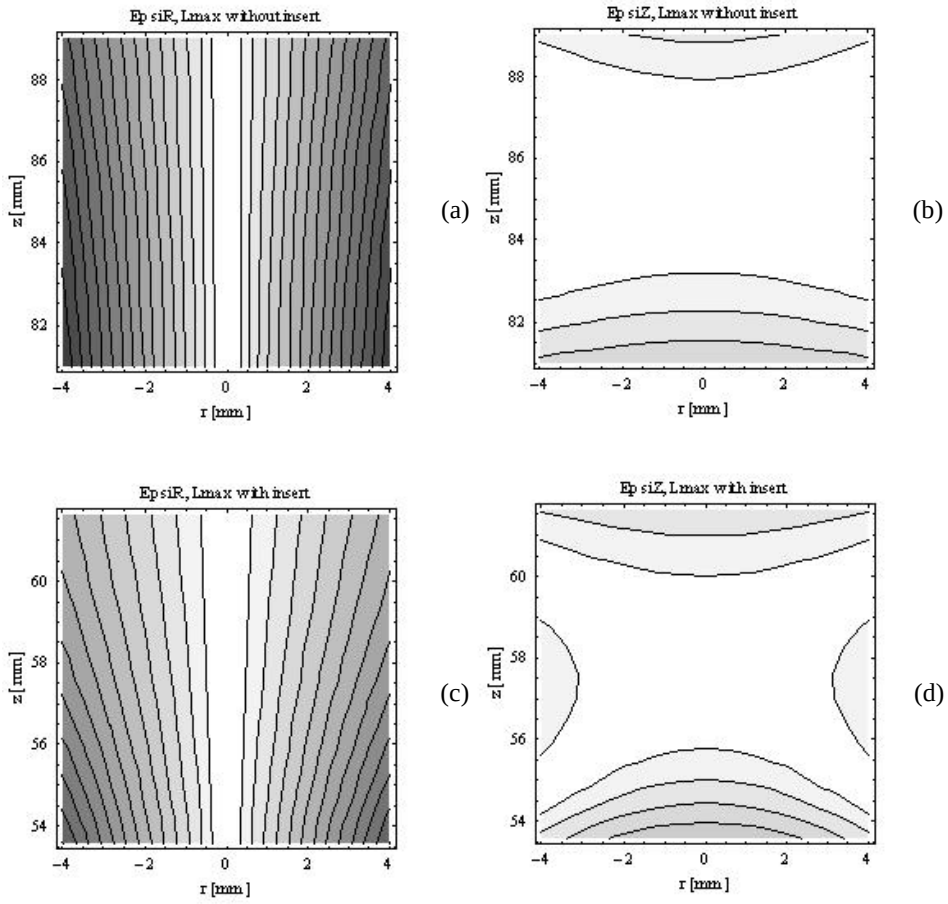

Fig. 4. L_{max} case : Contour plots of the radial homogeneity ε_r (a) and of the vertical homogeneity ε_z (b) in a window containing the working area without insert (Z_u = 85 mm). Contour plots of the radial homogeneity ε_r (c) and of the vertical homogeneity ε_z (d) in a window containing the working area with insert (Z_u = 57.6 mm).

Tab. III. Comparison of the levitation area location and of the required current density value needed to perform levitation with and without insert for both cases L_{equal} and L_{max}.

	L_{equal}		L_{max}	
	Without insert	With insert	Without insert	With insert
J (A/mm²)	189.3	195	188	194.1
I (A)	64.3	66.3	63.9	66
Z_u (mm)	90.8	62.3	85	57.6

Table IV. shows the comparison between the numerically calculated values of the magnetic flux density and the order of magnitude of the magnetic flux density derived from formula (21).

Tab. IV. Comparison of the calculation of the average magnetic flux density in the levitation area by using formula (21) and using numerical simulation for G=1000 T²/m and R=4 mm

	L_{equal}		L_{max}	
	Without insert	With insert	Without insert	With insert
ε_r (%)	2.9	1.6	3.6	2.1
ε_z (%)	2.9	1.6	0.6	0.7
$B_{simulation}$ (T)	6.2	8.0	6.6	8.3

$B_{formula}$ (T)	5.9	7.9	6.2	7.8

In the L_{equal} case, Table IV and Figure 3 point out that insert improves vertical and radial homogeneities. In the L_{max} case, only radial homogeneity is greatly improved by the insert.

Note the good correlation between the evaluation of *B* using formula (21) and the Radia calculation that checks the pertinence of the numerical evaluation.

4 Experimental results

In this section, experimental results are presented for three cases dealing with the behaviour of the liquid / gas phases at equilibrium coexistence. The phases are separated by an interface whose shape is very dependent on the amplitude of the different forces in presence. These forces are of capillary, gravity and magnetic origin. In order to reveal the residual magnetic and gravity forces, we will reduce as much as possible the capillary forces.

For this purpose, a closed H_2 sample is prepared at critical density, such as varying temperature enables the fluid to remain on the saturation line till its end point, the critical point. Below the critical point temperature T_c, the fluid shows up as two gas-liquid phases. Above T_c, the fluid is homogeneous, it is a gas at liquid density, a so-called "supercritical" fluid.

The vicinity of the critical point is accompanied by a number of important anomalies that will be used to detect the magnetic forces inhomogeneities. In particular, the gas-liquid surface tension σ goes to zero according to the power law $\sigma \sim (1-T/T_c)^{1.26}$ [4]. Therefore,

the capillary pressure (σ/R), which maintains spherical the gas bubble (radius R), will also go to zero. When going near the critical point under magnetic compensation of gravity, the shape of the bubble can then be deformed from an ideal sphere even by minute forces. The gas-liquid interface therefore tends to follow the force field lines and its shape will visualize the local force field inhomogeneities in a spectacular manner.

We will consider first the interface shape without magnetic field. Second, we present results under compensation without insert in the L_{max} case and, finally, consider compensation with insert in the L_{equal} case.

4.1 Test facility

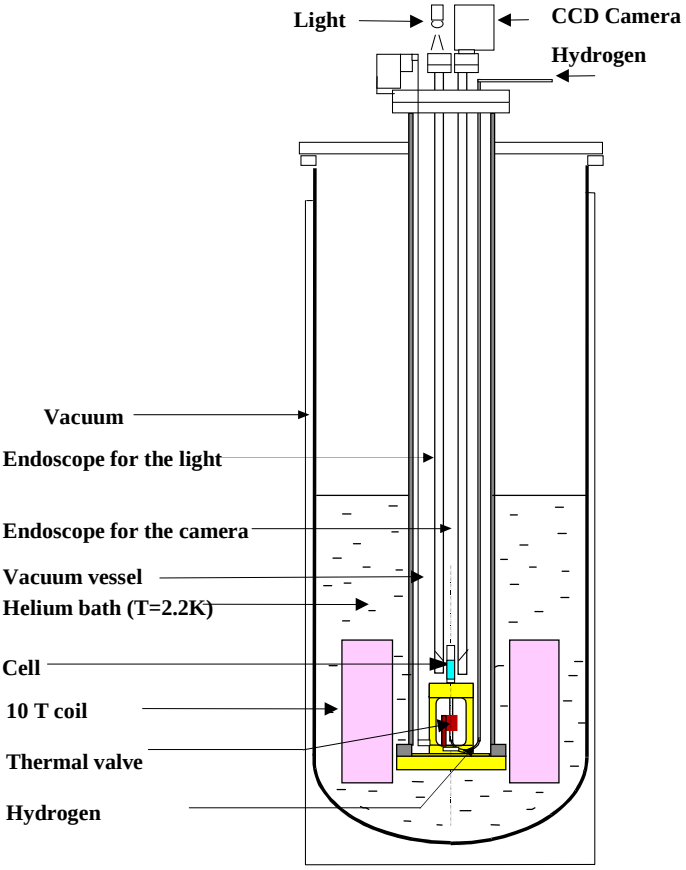

Fig. 5. Sketch of the experimental setup

The test facility (Fig. 5) consists in a superconductive solenoid immersed into a helium bath. The cell used was made of a copper cavity of 2 mm thickness and 8 mm in diameter closed by two sapphire windows of 24 mm in diameter and 2 mm thickness that permit direct observation (Fig. 6). These windows are fixed on the copper cavity with screws. Indium seals ensure the sealing of the cell. Observation of the levitation phenomena is performed with an endoscope and a CCD camera.

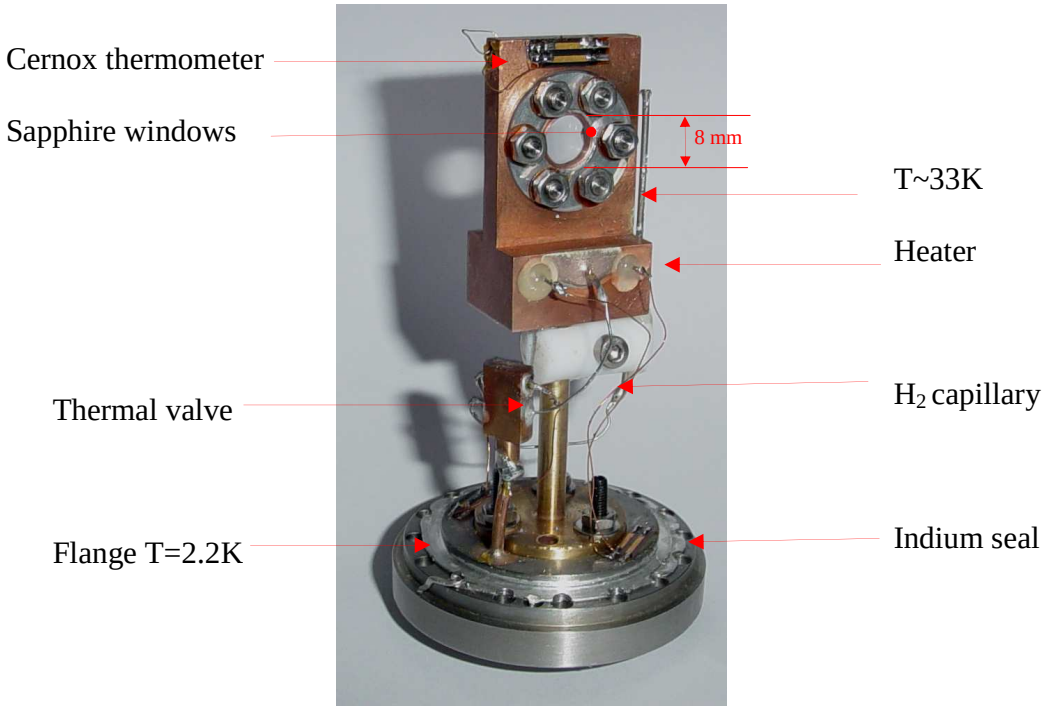

Fig. 6. A photograph of the 8 mm cell

The following operations are performed in order to compensate the gravity and levitate the hydrogen in the cell. (i) The system « cell + vacuum vessel » is placed into the cryostat; (ii) the vacuum vessel is pumped to about 10^{-6} mbar; (iii) the solenoid and the vacuum vessel are cooled down to 2.17K; (iv) the cell is heated to about 20K; (v) gaseous H_2 is slowly introduced into the cell by the capillary; (vi) when a sufficient quantity is condensed in the cell, heating of the valve is stopped so that an ice plug clogs up the capillary. (vii) the temperature of the cell is controlled; (viii) the current in the solenoid is increased to the required value to compensate gravity .

In the following, we will observe and analyse the shape of the vapour bubble. The photographs correspond to a front view of the cell.

4.2 Bubble interface without magnetic field

Figure 7 shows an example of the liquid / gas interface that can be observed in the cell (8 mm diameter) under earth gravity, at T = 20 K ($T-T_c$ = -13 K). Here the magnetic field is switched off. The liquid is located in the bottom and the gas at the top, surrounded by a gravity-thinned wetting layer. The shape of the meniscus corresponds to the competition between gravity forces, which tend to flatten the interface, and the capillary pressure, which tend to make the bubble spherical.

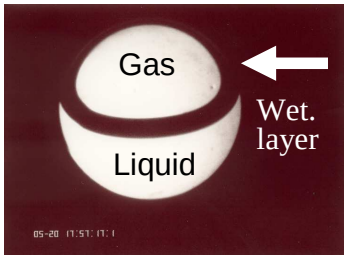

Fig. 7. Picture of the interface in a 8mm diameter cell without magnetic field at $T-T_c$ = -13 K.

4.3 Levitation without insert in the L_{max} case

The following Figure 8 shows a picture of the cell at the same temperature T = 20 K ($T-T_c$ = -13 K) under compensation of gravity.

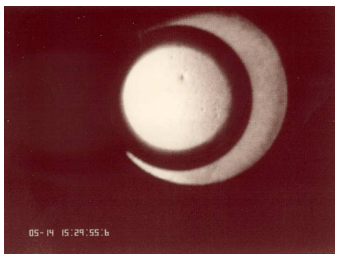

Fig. 8. Picture of the interface in a 8 mm cell

with magnetic field at $T-T_c = -13$ K. (L_{max} case)

Compensation is observed at $Z_u = 85$ mm and I = 63.9 A, which is in good agreement with the results of the calculation as reported in Table III. In the case of this experiment, performed far from the critical point, the surface tension forces dominate the residual magnetic forces. Consequently, the bubble shape is perfectly circular, as it would have been in actual weightlessness conditions. The bubble is close to a wall because of the radial centripetal forces. These forces make unstable the position where the vapour phase is on the coil symmetry axis.

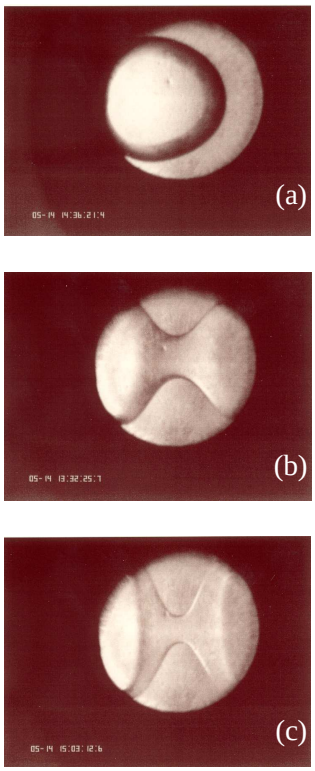

Fig. 9. Bubble shape close to T_c when a 8 mm diameter cell is used without insert. (a) $T-T_c$ = -500 mK. (b) $T-T_c$ = -20 mK. (c) $T-T_c$ = -10 mK. (L_{max} case)

Much closer to T_c [Figures 9(a), 9(b) and 9(c)], at $T-T_c$ = -500 mK, -20 mK and -10 mK, a progressive deformation of the liquid / gas interface from the spherical shape is observed. The deformations are the hall-mark of the magnetic residual forces. The radial components of the magnetic forces "push" the liquid towards the centre of the cell. It can easily be thus concluded that gravity is not homogeneously compensated. These results agree with the data of [4].

4.4 Levitation with insert in the L_{equal} case

In accord with the calculation of Table III, we have observed the gravity compensation at Z_u = 62 mm (62.3 mm expected) and for a current of I = 65.4 A.

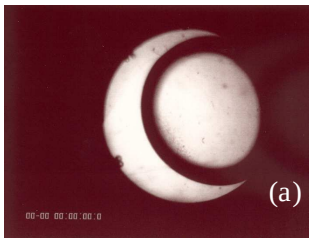

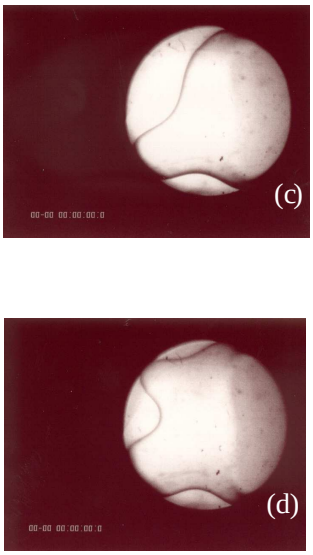

Fig. 10. Bubble shape close to T_c when a 8 mm diameter cell is used with insert. (a) $T-T_c$ = -500 mK. (b) $T-T_c$ = -20 mK. (c) $T-T_c$ = -10 mK. (d) $T-T_c$ = -5 mK. (L_{equal} case).

Figures 10(a), 10(b) and 10(c) show the bubble shape with gravity compensation with insert. In this case where $\varepsilon_r = \varepsilon_z$, the interface tends to keep a circular shape when the critical point is neared, which means that the residual forces are less important than without insert. At $T-T_c$ = -5 mK [Fig 10(d)], the deformation becomes important; however the liquid phase is still in contact with the walls.

5 Conclusions and perspectives

From mathematical arguments it thus comes out that is impossible to rigorously compensate gravity in a finished volume. The use of volumic magnetic forces is thus an

approximate technique to achieve gravity compensation. It is possible, however, to draw a relationship between the size of the volume to compensate, the residual inhomogeneities of the magnetic force field, the magnetic force value and the magnetic flux density in the levitation volume. This relationship highlights the fact that the homogeneity of the magnetic force and the dimensions of the levitation area are two parameters to take into account in any magnetic compensation device.

It appears that, in a classical coil, the force field homogeneity can be improved by the use of a ferromagnetic insert. Such an insert, after having been numerically calculated in the particular case of H_2 levitation in a 10 T superconducting coil, has been tested by observing the deviation from a sphere of the H_2 vapour phase very close to the critical point, where the surface tension goes to zero.

The results presented in this paper thus give a pertinent way to quickly evaluate the parameters of a given levitation problem. They allow the understanding of the intrinsic relationship between these parameters and the limits of the magnetic levitation technique to be quantitatively determined.

The experimental results presented in this paper are very encouraging and validate at the same time the methodology used to calculate the insert and the relevance of the association between a superconductive magnet and a ferromagnetic material in the levitation problems. Following this first stage, many prospects are thus open. In particular, it can be envisaged to develop new designs of insert and to use high critical temperature superconductors or materials with high saturation magnetic flux density at low temperature.

Acknowledgements

The authors gratefully acknowledge G Aubert (University J. Fourier, Grenoble) for his contribution concerning the demonstration of the relation (21). They thank D. Communal, T Jourdan, B Molinari, R Vallcorba and V. Nikolayev (CEA/SBT) for their contribution throughout this work.

References

[1] E. Beaugnon and R. Tournier, J. Phys. III, **8**, 1423-1428 (1991).

[2] M. V. Berry and A. K. Geim, J. Appl. Phys. **18**, 307-313 (1997).

[3] O. Ozaki, J. Fujihira, T. Kiyoshi, K. Koyanagi, S. Matsumoto, and H. Wada, MT 17, Geneva, (2001).

[4] R. Wunenburger, D. Chatain, Y. Garrabos, and D. Beysens, Phys. Rev. E, **62**, 469-476 (2000).

[5] L. Quettier and A. Mailfert, IEEE Trans. Appl. Super. **13**, 1608-1611 (2003).

[6] D. Beysens, D. Chatain, V. Nikolayev, Y. Garrabos, “Magnetic facility gives Heat transfer data in H2 at various acceleration levels” 4th International Conference on Launcher Technology "Space Launcher Liquid Propulsion"3-6 December 2002 Liege (Belgium) (2003)

[7] O. Vincent-Viry, L. Quettier, J. Leveque, A. Mailfert, and D. Chatain, IEEE Trans. Magn. **40**, 124 (2004).

[8] L. Quettier and A. Mailfert, in *Optimisation and Inverse Problems in Electromagnetism,* edited by M. Rudnicki and S. Wiak (Kluwer Academic Publishers, Dordrecht, 2003), Chap. 2, p.125, ISBN 1-4020-1506-2.

[9] G. Aubert, Private communication.

[10] P. Elleaume, O. Chubar, and J. Chavanne, Proc. Of PAC 97 Conference, 3509-3511, (1997).